(RNA) blots as described [M. J. Stewart and R. Denell, *Mol. Cell. Biol.* **13**, 2524 (1993)]. Plasmid rescue was as described [V. Pirrotta, in Drosophila, *a Practical Approach*, D. B. Roberts, Ed. (IRL Press, Oxford, UK, 1986), pp. 82–109]. Chimeric transcripts were reversed-transcribed with avian myeloblastosis virus (Promega) with an oligonucleotide priming from the exon 2 of the *dS6K* gene. PCR reaction products obtained revealed the presence of a chimeric mRNA containing the P-element sequence and the fusion of exon 1 to exon 2.

12. More severe alleles were obtained from the progeny of individual males carrying a Δ2-3 transposase and $dS6K^{07084}$ in trans with the deficiency Df(3L)64D-F [A. Garcia-Bellido, F. Cortes, M. Milan, *Proc. Natl. Acad. Sci. U.S.A.* **91**, 10222 (1994)], which did not complement the *dS6K* gene. Excision alleles were selected for their noncomplementation with the $dS6K^{07084}$ flies. To identify break points, we did PCR amplification from single flies [G. B. Gloor *et al.*, *Genetics* **135**, 81 (1993)], with oligonucleotides priming in the genomic sequence upstream of the P insertion point and in exon 8 of the *dS6K* gene.
13. The size of intervein cells was calculated by counting the number of hairs in a rectangle of 0.02 mm^2, located between veins 3 and 4 of the dorsal wing blade, up to the posterior cross vein. The total number of dorsal wing blade intervein cells was calculated by multiplying the number above by the area of the wing blade. For scanning electron microscopy, 3- to 4-day-old flies were anesthetized and immersed in 70% acetone. After critical point drying, they were mounted and coated with gold. The specimens were observed with a Hitachi S-800 field emission electron microscope at 6 kV.
14. M. Schubiger and J. Palka, *Dev. Biol.* **123**, 145 (1987) and (*26*), pp. 171–179. Female third instar wandering larvae were collected for disc dissection upon immobilization on the wall of the tube. Early prepupae were identified by spiracle eversion and before epidermal hardening. Wing disc cells were analyzed with a flow analysis cytometry sorter as described (3). The proliferation rate was estimated to be reduced by twofold by analyzing developing larvae. Four additional days were required to complete larval development and one additional day for pupation.
15. M. Madhavan and H. A. Schneiderman, *Wilhelm Roux's Arch.* **183**, 269 (1977).
16. A. Garcia-Bellido and J. R. Merriam, *Dev. Biol.* **24**, 61 (1971); M. J. Fain and B. Stevens, *ibid.* **92**, 247 (1982); B. J. Graves and G. Schubiger, *ibid.* **93**, 104 (1982).
17. F. C. Nielsen, L. Ostergaard, J. Nielsen, J. Christiansen, *Nature* **377**, 358 (1995); I. B. Leibiger, B. Leibiger, T. Moede, P. O. Berggren, *Mol. Cell* **1**, 933 (1998).
18. Somatic clones were generated with the FLP-FRT recombination system [T. Xu and G. M. Rubin, *Development* **117**, 1223 (1993)]. A 1-hour heat shock during the first larval instar permitted the recovery of clones in 50% of adults. Cross sections in eyes were performed as described [K. Basler, B. Christen, E. Hafen, *Cell* **64**, 1069 (1991)].
19. A. Garcia-Bellido, P. Ripoll, G. Morata, *Nature New Biol.* **245**, 251 (1973); D. Fristrom, M. Wilcox, J. Fristrom, *Development* **117**, 509 (1993).
20. N. Gorfinkiel, G. Morata, I. Guerrero, *Genes Dev.* **11**, 2259 (1997); F. J. Diaz-Benjumea and S. M. Cohen, *Cell* **75**, 741 (1993).
21. A. H. Brand and N. Perrimon, *Development* **118**, 401 (1993). Wing discs were dissected and stained with the D20 antibody (*27*) as described [U. G. Gaul, G. Mardon, G. M. Rubin, *Cell* **68**, 1007 (1992)].
22. When the wing blade is bent down such that it represents the arc of a quarter of a circle, the length of the dorsal wing sheet can be calculated from the equation $2L/\pi = (2L'/\pi) - d$, where L and L' represent the length of the ventral and dorsal wing sheets, respectively, and d is the distance between the middle of the two wing sheets. Because the length of the wing blade is 2 mm and the distance between the middle of the two wing sheets is about 10 μM [J. B. Tucker *et al.*, *Eur. J. Cell Biol.* **41**, 279 (1986)], the length of the dorsal sheet would measure 2.016 mm, a change of less than 1%.
23. P. B. Dennis, S. Fumagalli, G. Thomas, *Curr. Opin. Genet. Dev.* **9**, 49 (1999).
24. S. J. Leevers, D. Weinkove, L. K. MacDougall, E. Hafen, M. D. Waterfield, *EMBO J.* **15**, 6584 (1996).
25. M. Laser *et al.*, *J. Biol. Chem.* **273**, 24610 (1998).
26. M. Ashburner, Drosophila: *A Laboratory Manual* (Cold Spring Harbor Laboratory Press, Cold Spring Harbor, NY, 1989).
27. M. J. Stewart, C. O. A. Berry, F. Zilberman, G. Thomas, S. C. Kozma, *Proc. Natl. Acad. Sci. U.S.A.* **93**, 10791 (1996).

28. The authors thank W. Gehring, M. Jacobs-Lorena, W. Krek, K. Nasmyth, and M. Raff for fruitful discussions; J. Bailey-Serres, P. Caroni, P. B. Dennis, M. Hall, N. Pullen, and S. Volarevic for critical reading of the manuscript; J. Bailey-Serres for correcting the *dS6K* sequence; the Bloomington Stock Center for fly strains; M. Rothnie for the preparation of figures; A. Hefti for scanning electron micrographs; and M. Dessing for FACS analysis. M.J.S. was a recipient of an NIH National Research Service Award F32 GM15926, and this work was supported in part by a grant from the Swiss Cancer League to E.H., S.C.K., and G.T.

9 April 1999; accepted 11 August 1999

Affinity-Driven Peptide Selection of an NFAT Inhibitor More Selective Than Cyclosporin A

José Aramburu,[1,2] Michael B. Yaffe,[3] Cristina López-Rodríguez,[1,2] Lewis C. Cantley,[4] Patrick G. Hogan,[2,5]* Anjana Rao[1,2]*

The flow of information from calcium-mobilizing receptors to nuclear factor of activated T cells (NFAT)–dependent genes is critically dependent on interaction between the phosphatase calcineurin and the transcription factor NFAT. A high-affinity calcineurin-binding peptide was selected from combinatorial peptide libraries based on the calcineurin docking motif of NFAT. This peptide potently inhibited NFAT activation and NFAT-dependent expression of endogenous cytokine genes in T cells, without affecting the expression of other cytokines that require calcineurin but not NFAT. Substitution of the optimized peptide sequence into the natural calcineurin docking site increased the calcineurin responsiveness of NFAT. Compounds that interfere selectively with the calcineurin-NFAT interaction without affecting calcineurin phosphatase activity may be useful as therapeutic agents that are less toxic than current drugs.

Transcription factors of the NFAT family regulate immune responses as well as adaptive responses in heart and skeletal muscle (*1–3*). Four of the five NFAT proteins (NFAT1/p, NFAT2/c, NFAT3, and NFAT4/x) are cytoplasmic and are activated by stimulation of cell surface receptors coupled to Ca^{2+} mobilization (*1*). The Ca^{2+}-activated phosphatase calcineurin dephosphorylates these NFAT proteins, promoting their nuclear translocation and activation (*1*, *4*). Calcineurin docks at a site in the conserved NFAT regulatory domain that has the consensus sequence PxIxIT (*5*, *6*) (Fig. 1A). Interfering with docking of calcineurin at the PxIxIT sequence impairs NFAT activation and NFAT-dependent reporter gene expression (*5*).

To develop high-affinity NFAT inhibitors based on the PxIxIT sequence, we constructed combinatorial peptide libraries (*7*, *8*) (Fig. 1). The first library, with the sequence MA-xxxPxIxITxxHKK (where x represents a mixture of natural amino acid residues) was randomized in seven residues not fully conserved within the NFAT family (Fig. 1B). Peptides were selected for their ability to bind a glutathione S-transferase (GST) fusion protein containing the calcineurin catalytic domain (*8*). The peptide pool eluted from the calcineurin column showed moderate selection for glycine, serine, and lysine at position 3; no preferred residues at position 4; histidine or aliphatic residues at position 5; and moderate selection for polar residues (threonine, lysine, glutamine, and glutamic acid) at position 7 (Fig. 1B). Position 9 showed weak selection for aliphatic residues, notably valine. Glycine and proline were selected at positions 12 and 13, which suggests that the NFAT binding site in calcineurin imposes a turn at the COOH-terminal end of the PxIxIT motif.

To refine the peptide selection further, we

[1]Department of Pathology, Harvard Medical School; [2]The Center for Blood Research, 200 Longwood Avenue, Boston, MA 02115, USA. [3]Division of Signal Transduction, Departments of Medicine and Surgery, Beth Israel Deaconess Medical Center; [4]Division of Signal Transduction, Department of Medicine, Beth Israel Deaconess Medical Center, and Department of Cell Biology, Harvard Medical School, Harvard Institutes of Medicine, 330 Brookline Avenue, Boston, MA 02215, USA. [5]CBR Laboratories, 800 Huntington Avenue, Boston, MA 02115, USA.

*To whom correspondence should be addressed. E-mail: arao@cbr.med.harvard.edu (A.R.); hogan@cbr.med.harvard.edu (P.G.H.)

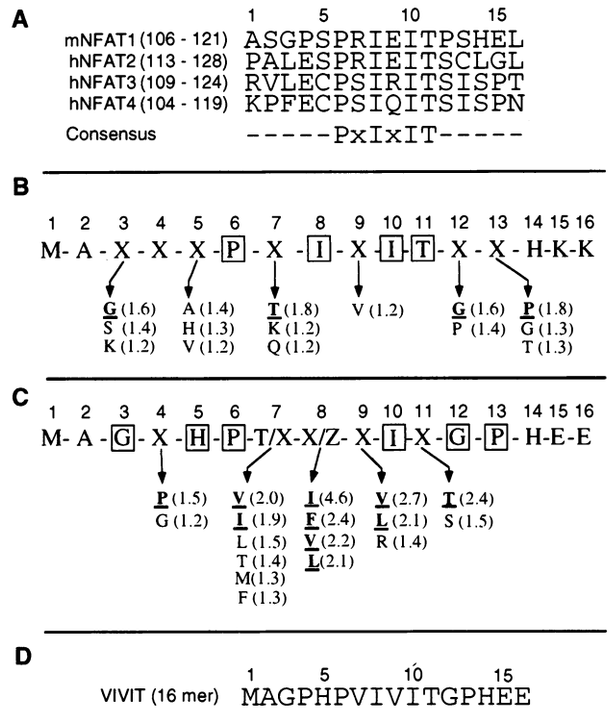

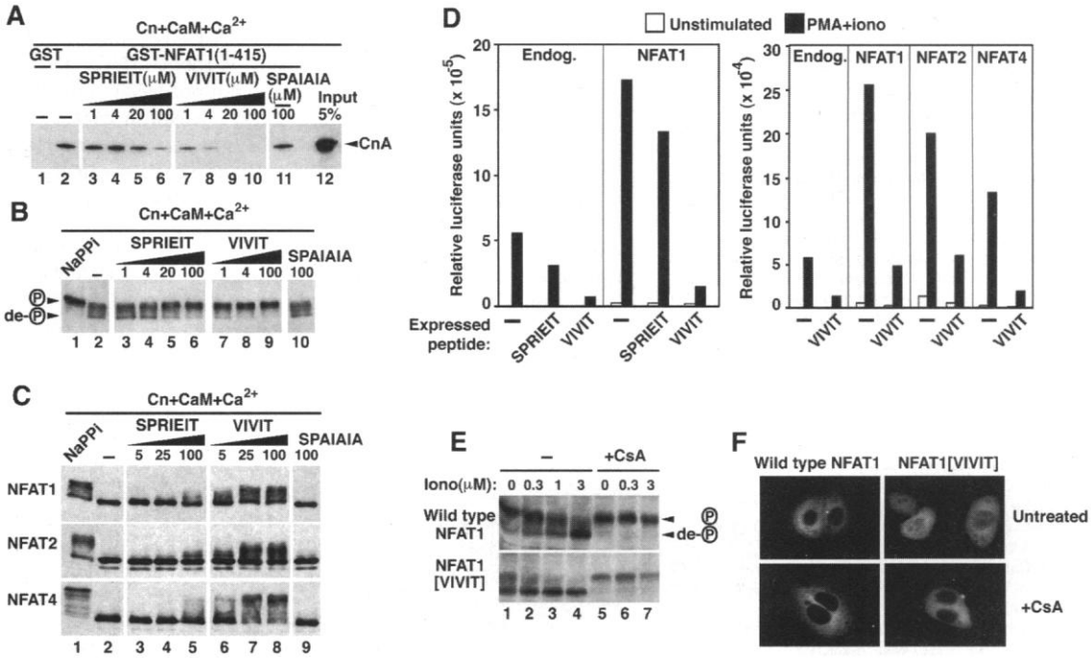

Fig. 1. Evolution of an optimized peptide that inhibits the NFAT-calcineurin interaction. (**A**) Calcineurin docking sequences present in NFAT family proteins. (**B**) First round of selection. A combinatorial peptide library anchored by the sequence PxIxIT from NFAT was selected by binding to GST-calcineurin (residues 2 through 347) (*8*). Positions fixed in the first (B) and second (C) degenerate peptide libraries are shown in the single-letter amino acid code, and randomized positions are indicated by X. Within the general library sequence, each X position contains roughly equimolar amounts of all amino acids except cysteine. Boxed residues are those conserved in all NFAT proteins. After extensive washing, the bound peptides were eluted and sequenced, and amino acids within each sequencing cycle were normalized to their abundance in the original library mixture. Particular amino acids selected in the degenerate positions are shown with preference values indicated in parentheses. Residues showing strong selection are shown bold and underlined. (**C**) Second round of selection. An alternative set of residues was chosen based on the initial screen (B) to orient a secondary library, and the second library was selected on GST-calcineurin (residues 2 through 347) to derive high-affinity peptides. Residues that were locked in based on the screening in (B) are boxed. Z indicates a member of a set of nonnatural amino acids (*8*). This screen revealed extremely strong selection for particular amino acids within the sequence, resulting in the optimal peptide VIVIT. (**D**) Sequence of the VIVIT peptide used in subsequent experiments. mer, oligomer.

Fig. 2. The VIVIT peptide is a potent inhibitor of the NFAT-calcineurin interaction, and its substitution into the calcineurin docking site enhances the calcineurin responsiveness of NFAT1. (**A**) Inhibition of the NFAT-calcineurin interaction (*9*). Calcineurin (Cn) was activated with calmodulin (CaM) and $CaCl_2$ (Ca^{2+}), and its binding to GST (lane 1) and GST-NFAT1 (residues 1 through 415) (lanes 2 through 11) was evaluated by protein immunoblotting. Cn A, calcineurin A chain. (**B** and **C**) Inhibition of the calcineurin-mediated dephosphorylation of NFAT proteins (*9*). Lysates of HeLa cells expressing HA-NFAT1 (B) or lysates from HEK 293T cells expressing HA-NFAT1, HA-NFAT2, or HA-NFAT4 (C) were incubated with the phosphatase inhibitor sodium pyrophosphate (NaPPi, lane 1) or with activated calcineurin (Cn+CaM+Ca^{2+}) in the absence or presence of peptides at the indicated micromolar concentrations. The phosphorylation status of NFAT proteins was evaluated by protein immunoblotting with anti-HA. The positions of phospho- and dephospho-NFAT are indicated by arrows in (B). (**D**) Inhibition of NFAT-dependent gene expression. (Left panel) Jurkat cells were cotransfected with a 3xNFAT-Luc reporter plasmid and with expression plasmids encoding murine NFAT1, GFP, GFP-SPRIEIT, or GFP-VIVIT as indicated (*13*). (Right panel) Jurkat cells were cotransfected with a 3xNFAT-Luc reporter plasmid and with expression plasmids encoding GFP, GFP-VIVIT, and murine NFAT1, human NFAT2, and human NFAT4 as indicated (*11*). Twenty-four hours after transfection, luciferase activity induced by endogenous NFAT (Endog.) or by overexpressed NFAT proteins was measured in unstimulated cells and in cells stimulated for 6 hours with PMA and ionomycin. (**E**) Substitution of the VIVIT sequence into NFAT1 (*12*). Cl.7W2 murine T cells were transfected with wild-type HA-NFAT1-GFP or with the mutant HA-NFAT1[VIVIT]-GFP, in which HPVIVITGP replaces SPRIEITPS. Cells were stimulated with ionomycin (Iono) at the concentrations indicated in the absence or presence of 1 μM CsA, and the phosphorylation status of NFAT1 was assessed by protein immunoblotting with anti-HA. (**F**) Localization of NFAT1 and NFAT1[VIVIT] in cells (*12*). HeLa cells transiently expressing wild-type HA-NFAT1-GFP or HA-NFAT1[VIVIT]-GFP were left untreated or were treated with 10 μM CsA (for 16 hours). NFAT1 proteins were visualized in fixed cells by GFP fluorescence.

used an affinity-driven peptide evolution technique (*7*). A second degenerate peptide library, MAGxHP[T/x][z/x]xIxGPHEE (where z represents a set of nonnatural residues) was synthesized, locking in some of the residues selected in the first screening while randomizing other positions that had been previously fixed (*8*) (Fig. 1C). Positions 3 and 5 were fixed as glycine and histidine; positions 12 and 13 were fixed as glycine and proline to favor the putative turn. Position 7 was biased to contain 50% threonine and 50% all other residues. Position 8 contained natural amino acid residues and five additional nonnatural amino acid residues with large aromatic or cyclic groups (*8*), to determine whether binding affinity could be improved by substituting a large hydrophobic side chain for the isoleucine side chain naturally conserved at this position in NFAT proteins. Position 10 was fixed as isoleucine, positions 9 and 11 were randomized, and the two COOH-terminal lysines were replaced by glutamates to prevent any bias produced by their positive charge.

Screening with the second library yielded strongly preferred residues at most of the randomized positions (Fig. 1C). The polar residues that occur naturally at the variable residues of the PxIxIT sequence in NFAT1-4 (R/S at position 7; E/R/Q at position 9) were not highly selected; rather, bulky or β-branched hydrophobic residues (valine, isoleucine, and leucine) were preferred. Proline was preferred at position 4, echoing its occurrence at this position of NFAT1 (but not NFAT2-4) (Fig. 1A). Isoleucine was stringently preferred at position 8, with lesser selection for other hydrophobic amino acids and no selection for the nonnatural amino acids, which is consistent with the invariance of isoleucine at this position of the PxIxIT sequence in all four NFAT proteins (Fig. 1A). Finally, there was strong selection for the conserved threonine at position 11 of the PxIxIT sequence, with a weaker preference for serine.

We synthesized the predicted optimal peptide MAGPHPVIVITGPHEE (*6*) (Fig. 1D) and examined its effect on the interaction of calcineurin with NFAT (*9*) (Fig. 2). This peptide (referred to hereafter as VIVIT) was about 25 times more effective than the original SPRIEIT peptide (*5*) at inhibiting the binding of activated calcineurin to GST-NFAT1 (Fig. 2A). The VIVIT peptide was also superior at inhibiting calcineurin-mediated dephosphorylation of NFAT1, NFAT2, and NFAT4 in cell extracts (Fig. 2, B and C). When expressed as a fusion protein with green fluorescent protein (GFP), the VIVIT peptide efficiently inhibited calcineurin-dependent nuclear translocation of NFAT1 (*10*) as well as activation of an NFAT-AP-1 reporter by endogenous or overexpressed NFAT1, NFAT2, and NFAT4 (*11*) (Fig. 2D). Thus, iterative peptide selection based on calcineurin binding yielded a highly inhibitory peptide, capable of disrupting all aspects of NFAT activation by calcineurin much more effectively than peptides spanning the natural calcineurin docking sequences of NFAT.

We asked whether substituting the high-

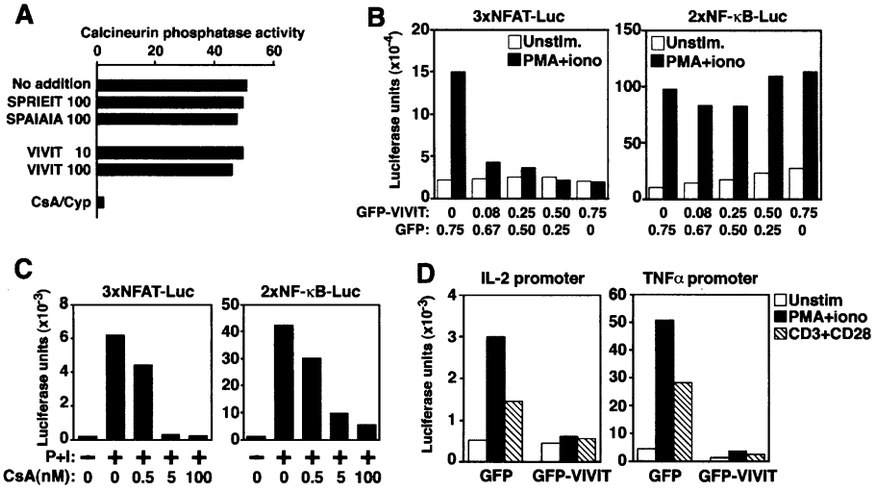

Fig. 3. The VIVIT peptide selectively inhibits NFAT activation but not calcineurin activity. (**A**) The VIVIT peptide did not inhibit calcineurin phosphatase activity, assayed as radiolabel released (counts per minute × 10^{-3}) from ^{32}P-phospho-RII peptide (*9*). The numbers next to each peptide label indicate peptide concentrations (micromolar). CsA/CypA complexes were used at 10 μM. (**B**) Selective inhibition of NFAT reporter activity (*11*). Jurkat cells were cotransfected with 3xNFAT-Luc (left panel) or 2xNF-κB-Luc (right panel) reporter plasmid, and with GFP and GFP-VIVIT expression plasmids as indicated (measured in micrograms of plasmid per 10^6 cells). Twenty-four hours after transfection, cells were left untreated (open bars) or were stimulated for 6 hours with PMA and ionomycin (solid bars). (**C**) Calcineurin dependence of NFAT and NF-κB reporter activity in T cells (*11*). Jurkat cells were transfected with 3xNFAT-Luc (left panel) or 2xNF-κB-Luc (right panel) reporter plasmid. Twenty-four hours after transfection, cells were left unstimulated or were stimulated for 6 hours with PMA and ionomycin (P+I) in the absence or presence of CsA. (**D**) Inhibition of NFAT-dependent activation of the IL-2 and TNF-α promoters (*11*). Jurkat cells were cotransfected with GFP or GFP-VIVIT expression plasmids and with luciferase reporter plasmids driven either by the human IL-2 promoter (left panel) or by the human TNF-α promoter (right panel). Twenty-four hours after transfection, cells were left unstimulated (open bars) or were stimulated for 6 hours with PMA and ionomycin (solid bars) or with anti-CD3 and anti-CD28 (hatched bars).

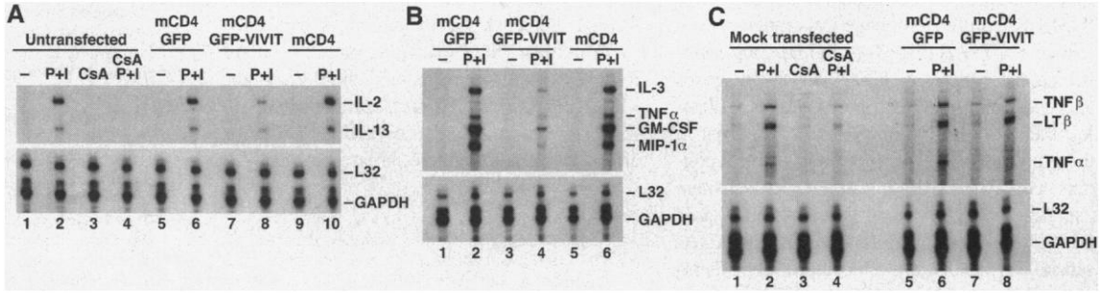

Fig. 4. The VIVIT peptide distinguishes NFAT-dependent and NFAT-independent categories of cyclosporin-sensitive genes. The expression of cytokine mRNAs by Jurkat T cells expressing mCD4 and GFP or GFP-VIVIT as indicated is shown (*13*). Cells were left unstimulated (dashes) or were stimulated for 3 hours with PMA and ionomycin (P+I) in the presence or absence of CsA, and levels of cytokine mRNAs were analyzed by RNase protection assay. RNA loading is indicated by the intensity of housekeeping transcripts L32 and GAPDH. (**A** and **B**) NFAT-dependent expression of IL-2, IL-13, IL-3, TNF-α, GM-CSF, and MIP-1α mRNAs. Autoradiogram exposure times were 24 hours (A) and 12 hours (B) for the upper panel and 4 hours (A) and 2 hours (B) for the lower panel. (**C**) NFAT-independent but CsA-sensitive expression of TNF-β and LT-β mRNAs. Exposure times were 36 hours for the upper panel and 12 hours for the lower panel.

affinity VIVIT sequence into a wild-type NFAT protein would increase its responsiveness to calcineurin. Compared to wild-type NFAT1, a mutant NFAT1[VIVIT] protein with the sequence SPRIEITPS replaced by HPVIVITGP (*12*) was significantly dephosphorylated even in resting cells and required lower concentrations of ionomycin to be fully dephosphorylated (Fig. 2E). Dephosphorylation of NFAT1[VIVIT] was calcineurin-dependent because it was blocked by cyclosporin A (CsA). Further, whereas wild-type NFAT1 was cytoplasmic in resting cells (Fig. 2F, left), NFAT1[VIVIT] consistently showed partial nuclear accumulation, which was prevented by CsA (Fig. 2F, right).

Inhibition of NFAT activation by the VIVIT peptide did not reflect inhibition at the calcineurin active site, because the peptide, at a concentration (100 μM) that effectively inhibited NFAT1-calcineurin binding and NFAT1 dephosphorylation (Fig. 2, A through C), did not inhibit calcineurin phosphatase activity toward the RII phosphopeptide (Fig. 3A). In the same experiment, CsA–cyclophilin A complexes (10 μM) inhibited calcineurin phosphatase activity by ~95% (Fig. 3A). Consistent with this observation, expression of the GFP-VIVIT fusion protein inhibited activation of an NFAT reporter but not of an NF-κB reporter (Fig. 3B), although both reporters were equivalently sensitive to inhibition of calcineurin with CsA (Fig. 3C). Thus, the VIVIT peptide selectively inhibits NFAT activation without disrupting other calcineurin-dependent pathways. GFP-VIVIT, but not GFP, inhibited reporter gene expression driven by the interleukin-2 (IL-2) and tumor necrosis factor α (TNF-α) promoters in T cells stimulated with phorbol ester (PMA) plus ionomycin or with antibody to CD3 (anti-CD3) plus anti-CD28 (Fig. 3D).

We tested the ability of the VIVIT peptide to inhibit expression of endogenous NFAT-dependent genes (Fig. 4). Jurkat cells highly enriched for expression of GFP-VIVIT or GFP (*13*) were stimulated and analyzed for cytokine expression by ribonuclease (RNase) protection assay. GFP-VIVIT inhibited the inducible expression of IL-2, IL-13, IL-3, TNF-α, granulocyte-macrophage colony-stimulating factor (GM-CSF) and macrophage inflammatory protein 1α (MIP-1α) (Fig. 4, A and B), thus establishing these genes as NFAT-dependent genes and confirming earlier reporter assays indicating the presence of functional NFAT sites in their promoter-enhancer regions (*1*). In contrast, GFP-VIVIT did not affect CsA-sensitive expression of TNF-β and lymphotoxin-β (LT-β) (Fig. 4C), establishing that there are CsA-sensitive (presumably calcineurin-dependent) genes that are not controlled by NFAT.

Our studies extend the range of experimental approaches for probing NFAT function in vivo. In addition to their established role in the immune response (*1*), NFAT and calcineurin have been implicated in cardiac and skeletal muscle hypertrophy (*2*, *3*), in slow fiber differentiation in skeletal muscle (*3*), in cardiac valve development (*14*), and in differentiation of a preadipocyte cell line to adipocytes in culture (*15*). These conclusions have relied on analysis of mouse models, identification of plausible NFAT sites in gene regulatory regions, expression of modified NFATs and calcineurins, and the use of CsA and FK506. The VIVIT peptide constitutes a highly selective inhibitor of NFAT, which can now be used for direct identification of NFAT target genes in these various cell types.

Substitution of the VIVIT sequence, a high-affinity calcineurin docking site, into wild-type NFAT1 causes it to be dephosphorylated and activated even in resting cells, which have low basal calcineurin activity. Evidently evolution has selected for an NFAT-calcineurin interaction of low to moderate affinity that precludes NFAT activation in resting cells. Our results call attention to the general point that many protein-protein interactions, especially those involving enzyme-substrate interactions or transient docking interactions (*16*), may be constrained to a range of low or moderate affinities in order to facilitate information transfer from one intracellular location to another, to ensure reversibility, and to prevent inappropriate activation at subthreshold levels of stimulus. The protein-protein interfaces involved in these reversible interactions would lend themselves to the design of small peptide or nonpeptide inhibitors.

The immunosuppressants CsA and FK506, used clinically to prevent transplant rejection, inhibit the phosphatase activity of calcineurin toward all its protein substrates, including NFAT (*1*). Although these drugs have revolutionized transplant therapy, their use is associated with progressive loss of renal function, hypertension, neurotoxicity, and increased risk of malignancy (*17*). It is not yet clear to what extent these toxicities are due to inhibition of NFAT, to interference with dephosphorylation of other calcineurin substrates, or to a potentially non–calcineurin-dependent up-regulation of TGF-β. Selective NFAT inhibitors will allow us to address these questions directly. NFAT inhibitors with less toxicity than CsA and FK506 could be useful in treating chronic ailments such as myocardial hypertrophy, allergy, arthritis, and autoimmune disease.

References and Notes

1. A. Rao, C. Luo, P. G. Hogan, *Annu. Rev. Immunol.* **15**, 707 (1997); C. López-Rodríguez, J. Aramburu, A. S. Rakeman, A. Rao, *Proc. Natl. Acad. Sci. U.S.A.* **96**, 7214 (1999); C. López-Rodríguez *et al.*, *Cold Spring Harbor Symp. Quant. Biol.*, in press; G. R. Crabtree, *Cell* **96**, 611 (1999).
2. J. D. Molkentin *et al.*, *Cell* **93**, 215 (1998); J. D. Molkentin, *Science* **282**, 1007 (1998); S. Izumo and H. Aoki, *Nature Med.* **4**, 661 (1998).
3. E. R. Chin *et al.*, *Genes Dev.* **12**, 2499 (1998). C. Semsarian *et al.*, *Nature* **400**, 576 (1999); A. Musaro, K. J. McCullagh, F. J. Naya, E. N. Olson, N. Rosenthal, *ibid.*, p. 581.
4. K. T.-Y. Shaw *et al.*, *Proc. Natl. Acad. Sci. U.S.A.* **92**, 11205 (1995); C. Luo *et al.*, *ibid.* **93**, 8907 (1996); F. Shibasaki, E. R. Price, D. Milan, F. McKeon, *Nature* **382**, 370 (1996); L. A. Timmerman, N. A. Clipstone, S. N. Ho, J. P. Northrop, G. R. Crabtree, *ibid.* **383**, 837 (1996); E. S. Masuda *et al.*, *Mol. Cell. Biol.* **17**, 2066 (1997).
5. J. Aramburu *et al.*, *Mol. Cell* **1**, 627 (1998); F. J. García-Cózar *et al.*, *J. Biol. Chem.* **273**, 23877 (1998).
6. Single-letter abbreviations for the amino acid residues are as follows: A, Ala; C, Cys; D, Asp; E, Glu; F, Phe; G, Gly; H, His; I, Ile; K, Lys; L, Leu; M, Met; N, Asn; P, Pro; Q, Gln; R, Arg; S, Ser; T, Thr; V, Val; W, Trp; x, any amino acid; and Y, Tyr.
7. M. B. Yaffe *et al.*, *Cell* **91**, 961 (1997).
8. Combinatorial peptide libraries were synthesized at the Tufts–New England Medical Center Peptide Synthesis Facility, using N-α-fluorenyl methoxycarbonyl–protected amino acids and standard BOP/HOBt coupling chemistry, as described previously (*7*). Within the general library sequence, each x position contains roughly equimolar amounts of all amino acids except cysteine. The nonnatural amino acids denoted as z in Fig. 1C were p-fluorophenylalanine, p-chlorophenylalanine, 2-naphthylalanine, tetrahydroisoquinoline-3-carboxylic acid, and cyclohexylalanine. Library screening was performed using ~1 mg of GST-calcineurin fusion protein that contained the calcineurin catalytic domain (residues 2 through 347), immobilized on 100 μl of glutathione-agarose resin in buffer containing 50 mM Hepes (pH 7.5), 150 mM NaCl, 5 mM $MgCl_2$, 300 μM $CaCl_2$, 100 μM sodium vanadate, 100 μM EGTA, 1 mM dithiothreitol, and 1% Triton X-100. After peptide binding, samples were washed twice with buffer and twice with phosphate-buffered saline, eluted with 30% acetic acid, and sequenced. Preference values for amino acids were determined by comparing the abundance of each amino acid at a particular position in the recovered peptides to that of the same amino acid at that position in the original peptide library mixture (*7*).
9. For the binding assays, calcineurin (Sigma) (200 nM) that had been activated with calmodulin (Sigma) (600 nM) and $CaCl_2$ (2 mM) was incubated with GST or with GST-NFAT1(1-415) (3 μg) (*5*). NFAT1-bound calcineurin was collected by incubation with glutathione-Sepharose resin and detected by protein immunoblotting with a polyclonal antibody to the calcineurin A chain (*18*). For the dephosphorylation assays, lysates of HeLa cells stably expressing HA-murine NFAT1(1-460)-GFP (briefly, HA-NFAT1) or HEK293T cells transfected with HA-NFAT1, human NFAT2 [HA-NFAT2 (1-418)], or human NFAT4 [HA-NFAT4(3-407)-GFP] were incubated with calcineurin (200 nM) plus calmodulin (600 nM) and $CaCl_2$ (2 mM). The phosphorylation status of NFAT was evaluated by protein immunoblotting with the antibody to HA 12CA5 (Boehringer Mannheim). The general phosphatase inhibitor sodium pyrophosphate was used at a 10 mM concentration. Calcineurin phosphatase activity was assayed by dephosphorylation of ^{32}P-labeled phospho-RII peptide (*5*). Under the conditions used (200 nM calcineurin and 20 min of incubation), calcineurin dephosphorylated ~60% of the input ^{32}P-RII peptide. For each of these assays, the peptides used as inhibitors were SPRIEIT-13 and SPAIAIA-25 (*5*), and the 16-oligomer VIVIT peptide (Fig. 1D).
10. J. Aramburu, unpublished data.
11. Jurkat cells were transfected (*5*, *19*) with luciferase reporter plasmids (0.25 μg per 10^6 cells) containing three tandem copies of the distal NFAT-AP-1 site of the murine IL-2 promoter (3xNFAT-Luc), two copies of a consensus NF-κB site (2xNF-κB-Luc), the human IL-2 promoter, or the human TNF-α promoter (*19*, *20*); with expression plasmids (0.25 μg per 10^6 cells) for NFAT1, NFAT2, NFAT4 (*5*, *21*); with a human growth hormone (hGH) plasmid as an internal reference for transfection efficiency (40 ng per 10^6 cells); and with GFP, GFP-SPRIEIT, or GFP-VIVIT expression plasmids (0.5 μg per 10^6 cells, or as indicated). The

GFP-VIVIT expression vector contained an oligonucleotide coding for MAGPHPVIVITGPHEE at the NH_2-terminus of GFP. Twenty-four hours after transfection, cells were stimulated for 6 hours with phorbol 12-myristate 13-acetate (PMA) (20 nM) and ionomycin (1 μM) or with immobilized anti-CD3 (0.2 μg/ml) (HIT3a, Pharmingen) and soluble anti-CD28 (0.5 μg/ml) (CD28.2, Pharmingen). CsA was added 30 min before the stimuli. Luciferase activity in cell lysates was normalized to levels of hGH.

12. The calcineurin targeting site of murine NFAT1, GPSPRIEITPSHELMQAGG (residues 108 through 126) was mutated to GPHPVIVITGPHELMQAGG (substitutions underlined) by replacing the DNA encoding the wild-type NFAT1 sequence between flanking Bsp 120I and Eco O109I sites with an oligonucleotide encoding the mutant sequence. Dephosphorylation of HA-NFAT1-GFP (*9*) was assessed in whole-cell extracts by protein immunoblotting, and subcellular localization was analyzed by GFP fluorescence (*5*).
13. Jurkat cells cotransfected with murine CD4 (mCD4) (0.75 mg per 10^6 cells) and GFP or GFP-VIVIT (0.75 μg per 10^6 cells) were selected with magnetic beads coated with anti-mCD4 (Dynabeads L3T4, Dynal, Lake Success, NY) (*22*). The selected mCD4-expressing cells were >90% GFP- or GFP-VIVIT–positive, whereas mCD4-nonexpressing cells were <5% GFP-positive, as assessed by fluorescence microscopy. Multiprobe RNase protection assays were performed with the RiboQuant multiprobe kit (Pharmingen) (*22*).
14. A. M. Ranger *et al.*, *Nature* **392**, 186 (1998); J. L. de la Pompa *et al.*, *ibid.*, p. 182.
15. I.-C. Ho, J. H.-J. Kim, J. W. Rooney, B. M. Spiegelman, L. H. Glimcher, *Proc. Natl. Acad. Sci. U.S.A.* **95**, 15537 (1998).
16. A. C. Greenlund *et al.*, *Immunity* **2**, 677 (1995); U. Schindler, P. Wu, M. Rothe, M. Brasseur, S. L. McKnight, *ibid.*, p. 689; T. Tsukazaki, T. A. Chiang, A. F. Davison, L. Attisano, J. L. Wrana, *Cell* **95**, 779 (1998); L. Attisano and J. L. Wrana, *Curr. Opin. Cell Biol.* **10**, 188 (1998); T. Kallunki, T. Deng, M. Hibi, M. Karin, *Cell* **87**, 929 (1996); A. J. Whitmarsh, J. Cavanagh, C. Tournier, J. Yasuda, R. J. Davis, *Science* **281**, 1671 (1998).
17. N. H. Sigal *et al.*, *J. Exp. Med.* **173**, 619 (1991); M. Pascual *et al.*, *Immunol. Today* **11**, 514 (1998). M. Hojo *et al.*, *Nature* **397**, 530 (1999); G. J. Nabel, *ibid.*, p. 471; M. J. Mihatsch *et al.*, *Clin. Nephrol.* **49**, 356 (1998); M. Cecka, *Surg. Clin. North. Am.* **78**, 133 (1998).
18. C. Loh *et al.*, *J. Biol. Chem.* **271**, 10884 (1996).
19. C. Luo *et al.*, *Mol. Cell. Biol.* **16**, 3955 (1996).
20. F. Mercurio *et al.*, *Science* **278**, 860 (1997).
21. J. P. Northrop *et al.*, *Nature* **369**, 497 (1994); T. Hoey, Y. L. Sun, K. Williamson, X. Xu, *Immunity* **2**, 461 (1995).
22. A. Kiani, J. P. B. Viola, A. H. Lichtman, A. Rao, *Immunity* **7**, 849 (1997).

23. We thank M. Berne for peptide synthesis and sequencing; D. Littman, G. Crabtree, and T. Hoey for reagents; and members of the laboratory for helpful discussion and advice. Supported by NIH grants R01 AI 40127 (to A.R.), R43 AI 43726 (to P.G.H.), R01 HL 03601 (to M.B.Y.), and R01 GM 56203 (to L.C.C.); by the Ministerio de Educación y Ciencia, Spain (C.L.-R.); and by the Arthritis Foundation (J.A.).

3 June 1999; accepted 24 August 1999

Identification of an RNA-Protein Bridge Spanning the Ribosomal Subunit Interface

Gloria M. Culver,* Jamie H. Cate,† G. Zh. Yusupova, Marat M. Yusupov, Harry F. Noller‡

The 7.8 angstrom crystal structure of the 70*S* ribosome reveals a discrete double-helical bridge (B4) that projects from the 50*S* subunit, making contact with the 30*S* subunit. Preliminary modeling studies localized its contact site, near the bottom of the platform, to the binding site for ribosomal protein S15. Directed hydroxyl radical probing from iron(II) tethered to S15 specifically cleaved nucleotides in the 715 loop of domain II of 23*S* ribosomal RNA, one of the known sites in 23*S* ribosomal RNA that are footprinted by the 30*S* subunit. Reconstitution studies show that protection of the 715 loop, but none of the other 30*S*-dependent protections, is correlated with the presence of S15 in the 30*S* subunit. The 715 loop is specifically protected by binding free S15 to 50*S* subunits. Moreover, the previously determined structure of a homologous stem-loop from U2 small nuclear RNA fits closely to the electron density of the bridge.

Ribosomes are large ribonucleoprotein complexes that are responsible for the fundamental process of protein synthesis. They are composed of two asymmetric subunits, each of which contributes to specific functions during translation. The interface between these subunits allows for the coordination of these discrete functions and also provides the binding surfaces for many substrates and ligands. Thus, the identification of specific molecular interactions between the two subunits is of great importance. Numerous experiments have identified RNA and protein elements that potentially contribute to this subunit-subunit interface (*1*–*3*). However, in the absence of high-resolution structural information, identification of the molecular components comprising specific subunit-subunit interactions has been difficult.

The 7.8 Å x-ray crystal structure of the *Thermus thermophilus* 70*S* ribosome (*4*) shows that the two ribosomal subunits are connected by a complex network of molecular interactions. One of these (bridge B4) can be identified as a double-stranded RNA stem-loop that is continuous with the 50*S* subunit and makes contact with the bottom of the platform of the 30*S* subunit (Fig. 1). Immunoelectron microscopy and preliminary modeling studies of the 30*S* subunit based on extensive biochemical, biophysical, and phylogenetic evidence localize the binding site for protein S15 to this region of the 30*S* subunit (*5*). Additionally, evidence for the placement of S15 at the subunit interface has come from intersubunit cross-linking studies (*2*) and a temperature-sensitive S15 mutant that is defective in subunit association (*6*).

To test the possible proximity of S15 to 23*S* ribosomal RNA (rRNA), we performed directed hydroxyl radical probing (*7*). Iron(II) was tethered by a linker, 1-(*p*-bromoacetamidobenzyl)-EDTA (BABE) (*8*), to unique cysteine (C) residues on the surface of S15 at amino acid positions 12, 36, 46, and 70 by directed mutagenesis (*9*), using the published solution and crystal structures of S15 as a guide (*10*). The Fe(II)-derivatized proteins were incorporated into 30*S* subunits by in vitro reconstitution (*11*) and associated with 50*S* subunits to form 70*S* ribosomes, which were then purified by sucrose gradient centrifugation. The 30*S* subunits containing S15 derivatized at position 70 failed to associate with 50*S* subunits, although they appeared to be normally as-

Fig. 1. Electron density from the 7.8 Å crystal structure of the *T. thermophilus* 70*S* ribosome (*4*) showing interaction of a discrete RNA feature of the 50*S* subunit (white) with the bottom of the platform of the 30*S* subunit (blue). Electron density is contoured at 1.1σ.

Center for Molecular Biology of RNA, Sinsheimer Laboratories, University of California, Santa Cruz, CA 95064, USA.

*Present address: Department of Biochemistry, Biophysics, and Molecular Biology, Iowa State University, Ames, IA 50011, USA.

†Present address: Whitehead Institute for Biomedical Research and Massachusetts Institute of Technology, Cambridge, MA 02142, USA.

‡To whom correspondence should be addressed.

http://www.jstor.org

LINKED CITATIONS

- Page 1 of 2 -

You have printed the following article:

Affinity-Driven Peptide Selection of an NFAT Inhibitor More Selective Than Cyclosporin A

Jose Aramburu; Michael B. Yaffe; Cristina Lopez-Rodriguez; Lewis C. Cantley; Patrick G. Hogan; Anjana Rao

Science, New Series, Vol. 285, No. 5436. (Sep. 24, 1999), pp. 2129-2133.

Stable URL:

http://links.jstor.org/sici?sici=0036-8075%2819990924%293%3A285%3A5436%3C2129%3AAPSOAN%3E2.0.CO%3B2-6

This article references the following linked citations:

References and Notes

[4] **Immunosuppressive Drugs Prevent a Rapid Dephosphorylation of Transcription Factor NFAT1 in Stimulated Immune Cells**

Karen T.-Y. Shaw; Andrew M. Ho; Anuradha Raghavan; Jaime Kim; Jugnu Jain; Jungchan Park; Surendra Sharma; Anjana Rao; Patrick G. Hogan

Proceedings of the National Academy of Sciences of the United States of America, Vol. 92, No. 24. (Nov. 21, 1995), pp. 11205-11209.

Stable URL:

http://links.jstor.org/sici?sici=0027-8424%2819951121%2992%3A24%3C11205%3AIDPARD%3E2.0.CO%3B2-9

[4] **Interaction of Calcineurin with a Domain of the Transcription Factor NFAT1 that Controls Nuclear Import**

Chun Luo; Karen T.-Y. Shaw; Anuradha Raghavan; Jose Aramburu; Francisco Garcia-Cozar; Brian A. Perrino; Patrick G. Hogan; Anjana Rao

Proceedings of the National Academy of Sciences of the United States of America, Vol. 93, No. 17. (Aug. 20, 1996), pp. 8907-8912.

Stable URL:

http://links.jstor.org/sici?sici=0027-8424%2819960820%2993%3A17%3C8907%3AIOCWAD%3E2.0.CO%3B2-R

[15] **A Potential Role for the Nuclear Factor of Activated T Cells Family of Transcriptional Regulatory Proteins in Adipogenesis**

I-Cheng Ho; John H.-J. Kim; John W. Rooney; Bruce M. Spiegelman; Laurie H. Glimcher

Proceedings of the National Academy of Sciences of the United States of America, Vol. 95, No. 26. (Dec. 22, 1998), pp. 15537-15541.

Stable URL:

http://links.jstor.org/sici?sici=0027-8424%2819981222%2995%3A26%3C15537%3AAPRFTN%3E2.0.CO%3B2-1

NOTE: *The reference numbering from the original has been maintained in this citation list.*

http://www.jstor.org

LINKED CITATIONS

[16] **A Mammalian Scaffold Complex That Selectively Mediates MAP Kinase Activation**
Alan J. Whitmarsh; Julie Cavanagh; Cathy Tournier; Jun Yasuda; Roger J. Davis
Science, New Series, Vol. 281, No. 5383. (Sep. 11, 1998), pp. 1671-1674.
Stable URL:
http://links.jstor.org/sici?sici=0036-8075%2819980911%293%3A281%3A5383%3C1671%3AAMSCTS%3E2.0.CO%3B2-Q

[20] **IKK-1 and IKK-2: Cytokine-Activated IkB Kinases Essential for NF- kB Activation**
Frank Mercurio; Hengyi Zhu; Brion W. Murray; Andrej Shevchenko; Brydon L. Bennett; Jian wu Li; David B. Young; Miguel Barbosa; Matthias Mann; Anthony Manning; Anjana Rao
Science, New Series, Vol. 278, No. 5339. (Oct. 31, 1997), pp. 860-866.
Stable URL:
http://links.jstor.org/sici?sici=0036-8075%2819971031%293%3A278%3A5339%3C860%3AIAICIK%3E2.0.CO%3B2-B

NOTE: *The reference numbering from the original has been maintained in this citation list.*